Exposing inequitable risk estimation of emergency service disruptions during urban floods

Supplementary Information

Xiyu Pan[1], Neda Mohammadi[1,2], John E. Taylor[1, *]

[1] School of Civil and Environmental Engineering, Georgia Institute of Technology, 790 Atlantic Dr NW, Atlanta, GA, 30332, USA

[2] Faculty of Engineering, The University of Sydney, NSW 2006, Australia

Supplementary Figures:

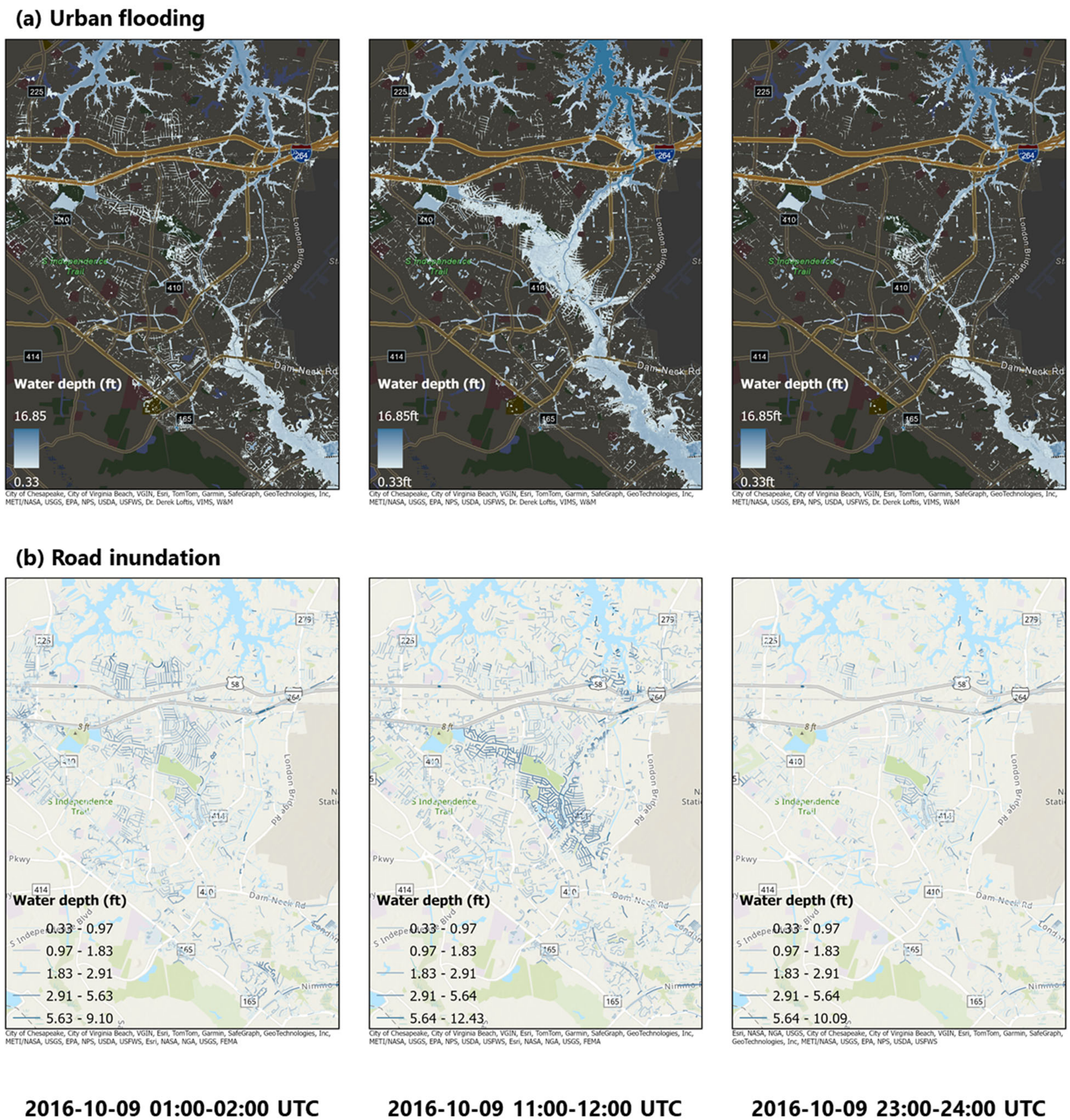

Figure S1. Estimated (a) urban flooding and (b) road inundation maps for Virginia Beach, VA at selected periods. 11:00-12:00 UTC was the peak of the urban flooding, and the other two periods were close to the beginning and end of the flood simulation.

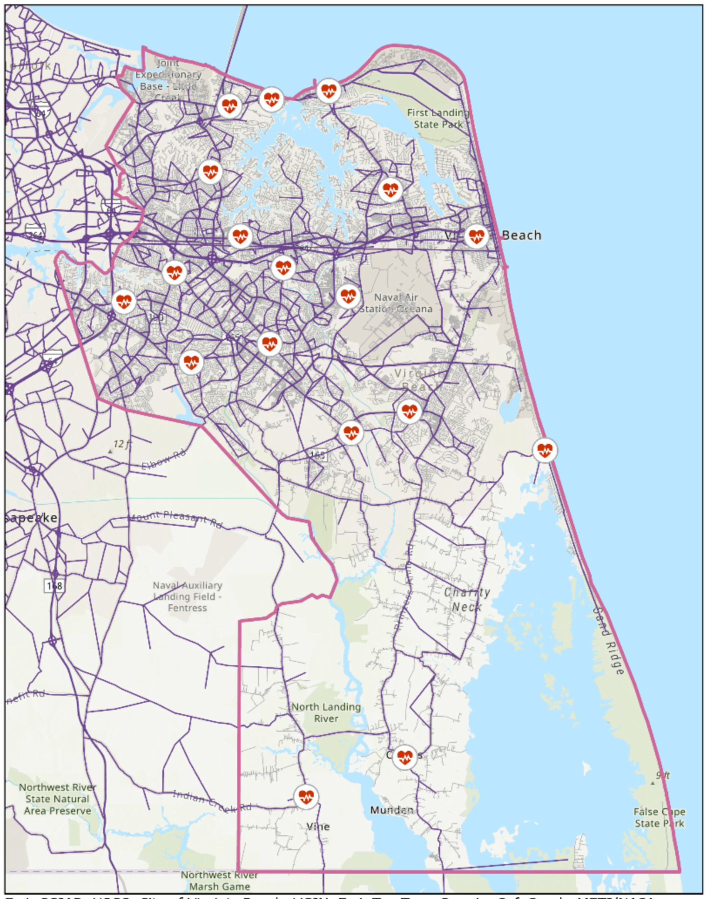

Esri, CGIAR, USGS, City of Virginia Beach, VGIN, Esri, TomTom, Garmin, SafeGraph, METI/NASA, USGS, EPA, NPS, USDA, USFWS

Figure S2. Map of Virginia Beach, VA with the city boundary, locations of emergency service stations, major roads in purple, and side roads in grey.

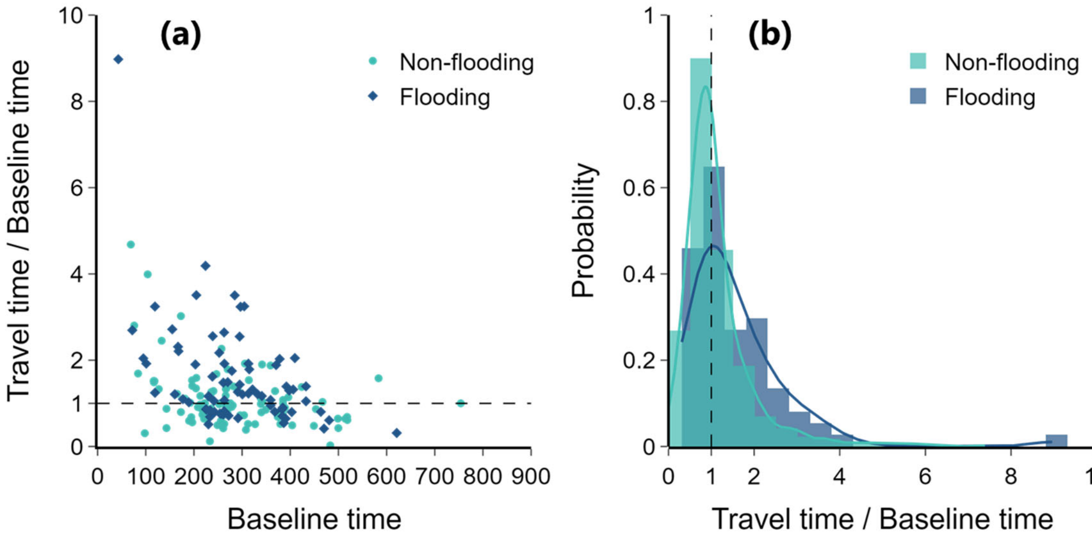

Figure S3. Normalized travel time of ambulances in flooding and non-flooding periods based on the real-world dataset. The normalized travel time is the ratio of the travel time of an incident over the corresponding baseline time. The baseline is defined as the average travel time of all incidents at the same spot during the non-flooding period. (a) is the normalized travel time versus the baseline time, and (b) is the histogram of the normalized travel time with kernel density estimation curve. Zero travel time and travel time out of the $\pm 3\sigma$ range were regarded as incorrect records and were excluded. One hundred non-flooding incidents and one thousand non-flooding incidents were randomly sampled for (a) and (b), respectively, for better visualization. Normalized travel time over 10 were excluded for better visualization in (b).

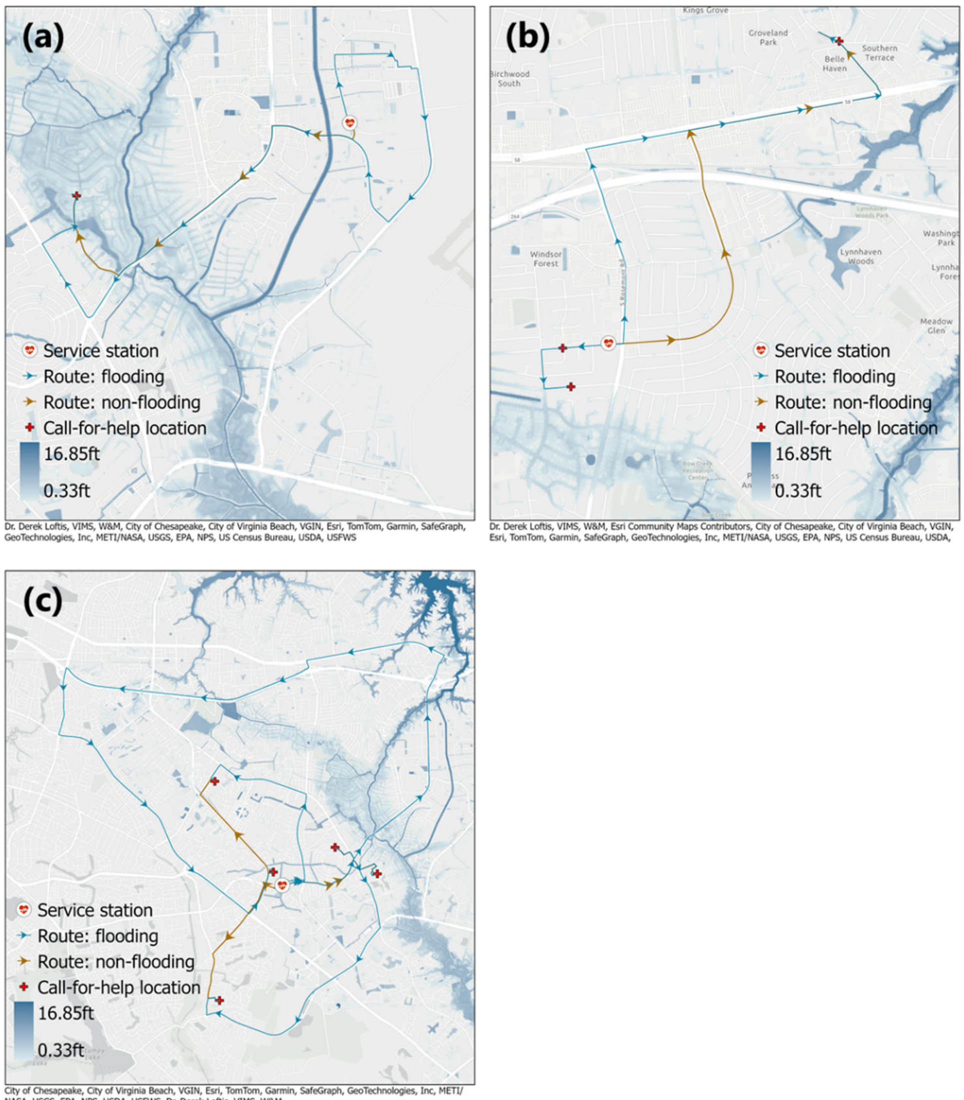

Figure S4. Results of the quickest routing during the flooding and non-flooding periods at (a) Station R03, (b) Station R16, and (c) Station R18. These three stations were selected because they were closest to the flooding center. The call-for-help locations in the figure are those seeing call-for-help during both the flooding and non-flooding periods.

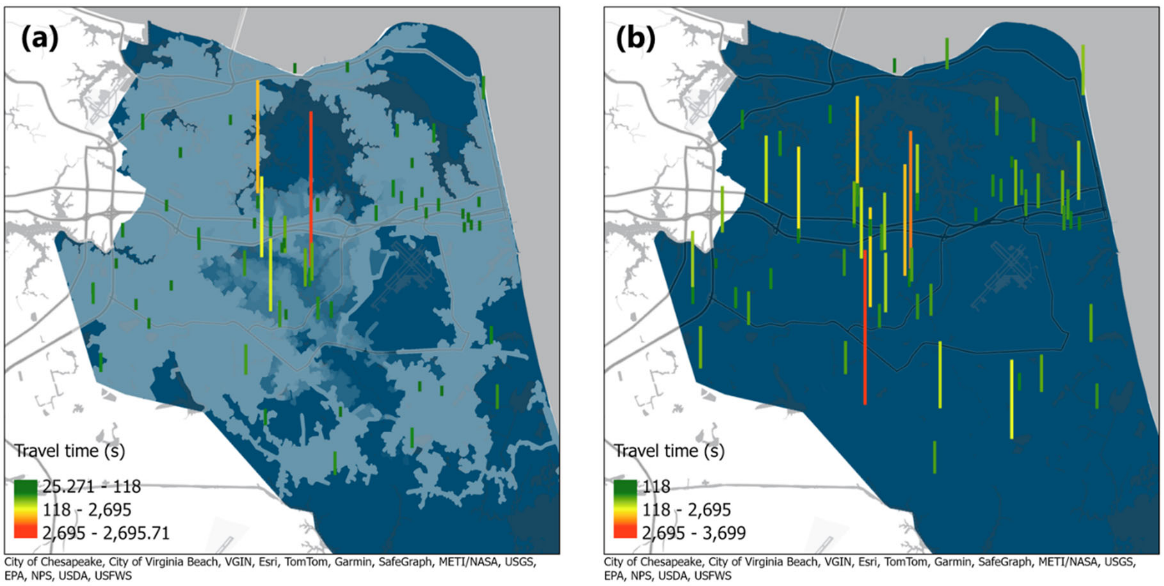

Figure S5. (a) Estimated travel time and service areas of EMS during the flooding day and the (b) ground truth travel time. The overlapping white polygons with transparency are the 324-second service area of all available emergency service stations at different hours (sampled every other hour in the flooding day). Please refer to Methods for the reason of 324s threshold. The service areas are overlapping, and darker color (i.e., the background dark blue) indicates lower level of service coverage.

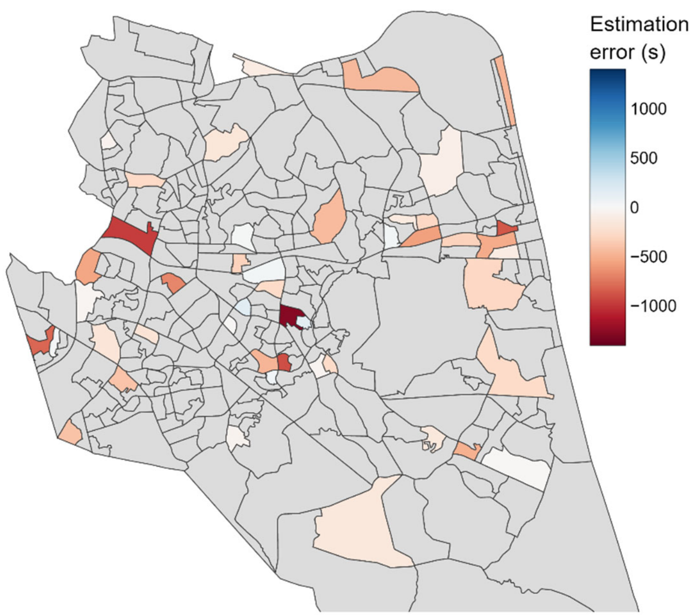

Figure S6. Average ambulance travel time estimation errors on the block group level. Negative values are underestimation and grey polygons indicate no EMS calls during the flooding day.

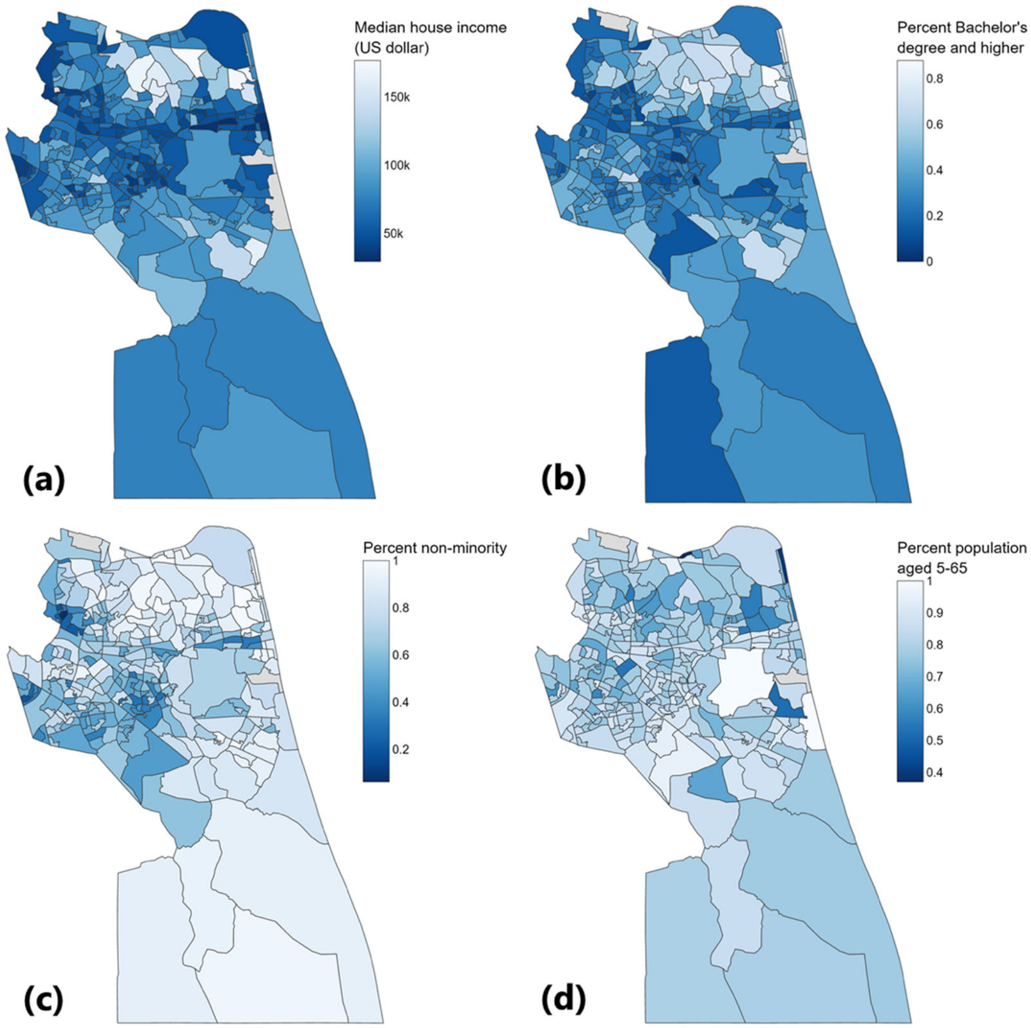

Figure S7. Spatial distributions of (a) income, (b) education, (c) minority, and (d) vulnerable age metric values in Virginia Beach, VA, at the block group level. Grey polygons indicate missing records in the data source.

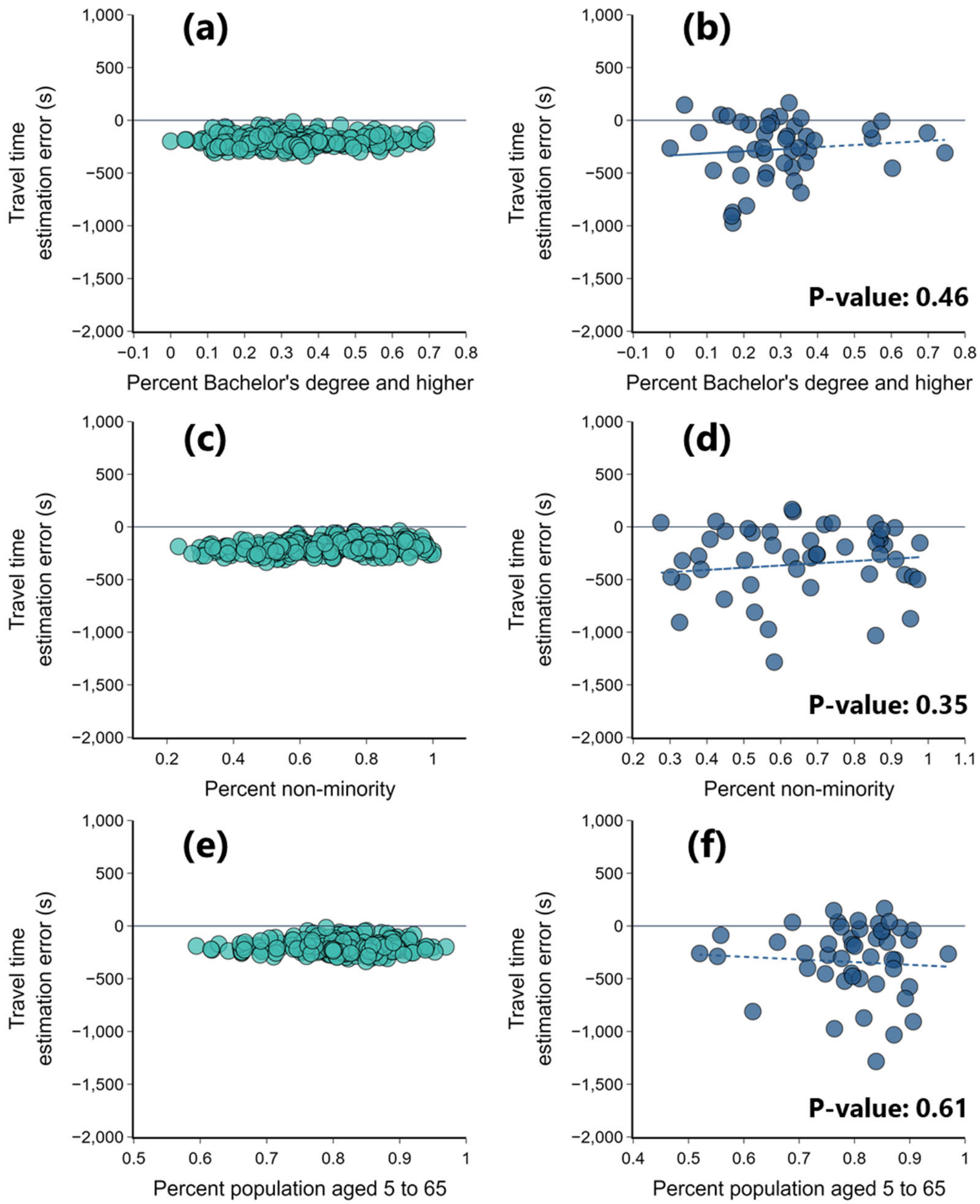

Figure S8. Emergency service travel time estimation errors versus (a-b) education, (c-d) minority, and (e-f) age vulnerability metric values during the non-flooding and flooding periods. Each point represents a block group under study. Dashed trend lines and the p-values for the non-zero slope hypothesis are the results from the spatial regression model introduced in the Methods.

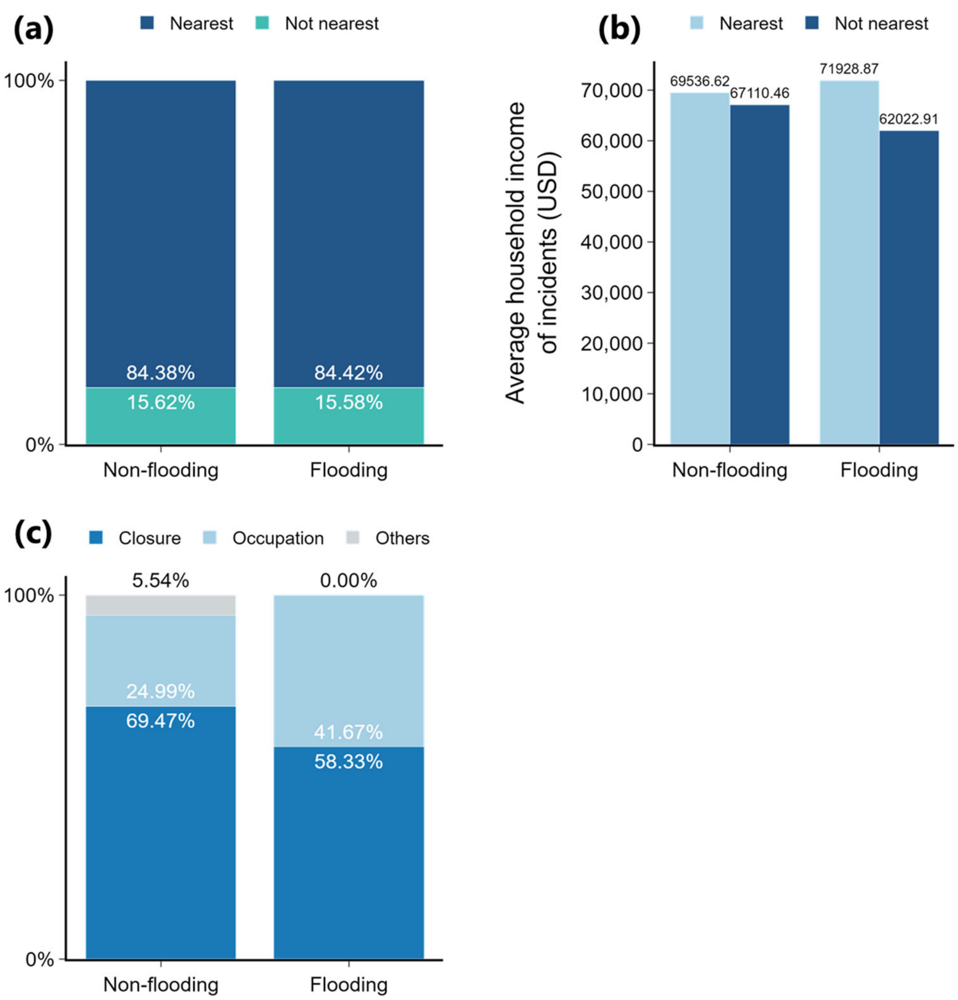

Figure S9. Non-nearest EMS dispatches and their relationships to economic status. (a) shows the percentage of the nearest and non-nearest dispatches, and (b) illustrates the average household income of the incidents handled by nearest and non-nearest dispatches. The household income of each incident is the median household income of the block group it belongs to. (c) demonstrates the reasons for the non-nearest dispatches.

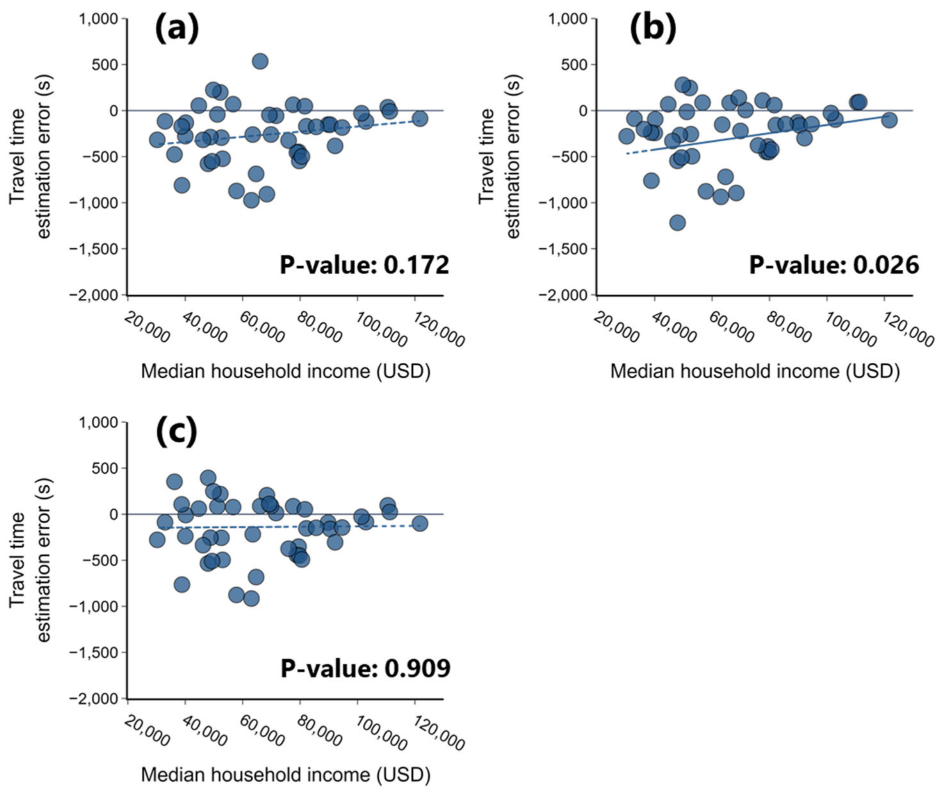

Figure S10. Income versus travel time estimation error for each block group when considering (a) recorded service station matches, (b) non-flooding period daily traffic congestions, and (c) the flooding day cascading congestions.

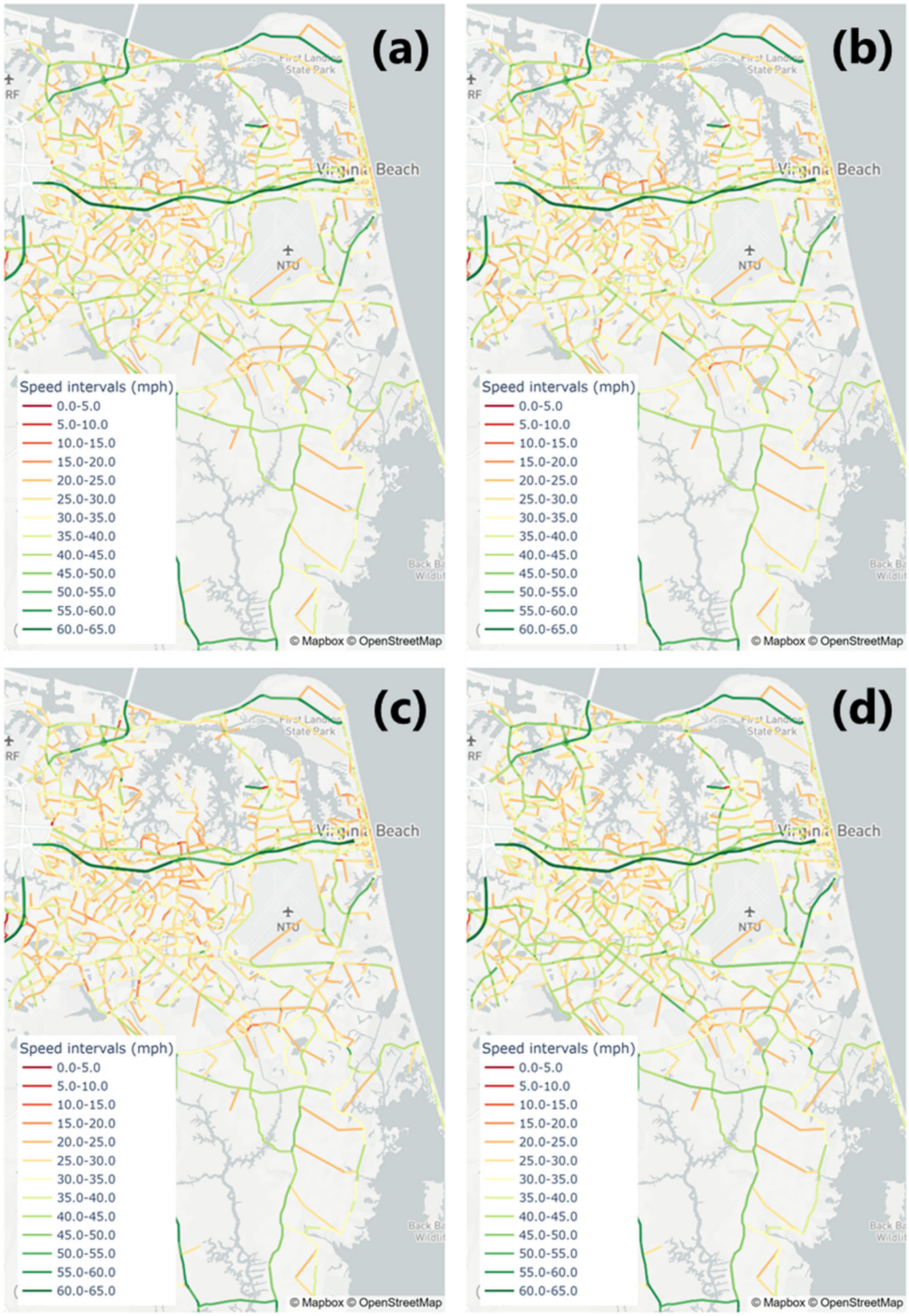

Figure S11. Simulated traffic speed map for Virginia Beach, VA during the non-flooding time when (a) the morning peak time (i.e., 5 AM to 9 AM), (b) the midday off-peak time (i.e., 9 AM to 3 PM), (c) the evening peak time (i.e., 3 PM to 6 PM), and (d) the night off-peak time (6 PM to 5 AM).

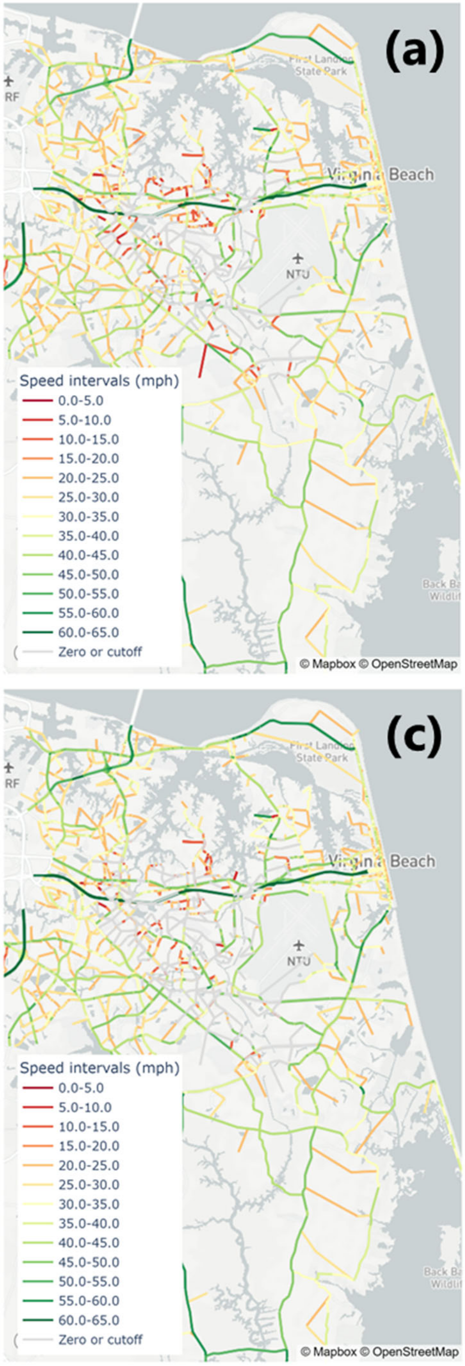

Figure S12. Simulated traffic speed map for Virginia Beach, VA during the flooding day when (a) the morning peak time (i.e., 5 AM to 9 AM), (b) the midday off-peak time (i.e., 9 AM to 3 PM), and (c) the night off-peak time (6 PM to 5 AM). Please refer to Figure 3 for the map when the evening peak time (i.e., 3 PM to 6 PM).

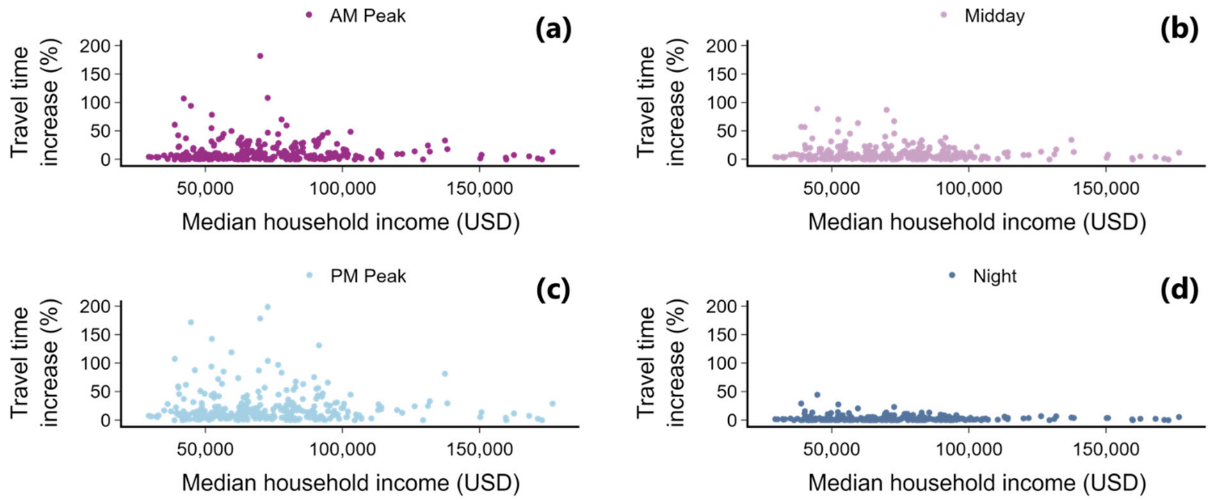

Figure S13. Block groups' median household income and flooding day travel time increase percentages over the free flow scenario when (a) the morning peak time (i.e., 5 AM to 9 AM), (b) the midday off-peak time (i.e., 9 AM to 3 PM), (c) the evening peak time (i.e., 3 PM to 6 PM), and (d) the night off-peak time (6 PM to 5 AM). The travel time increase percentage considers all modeled road segments in each block group except for the roads cut off by inundations.

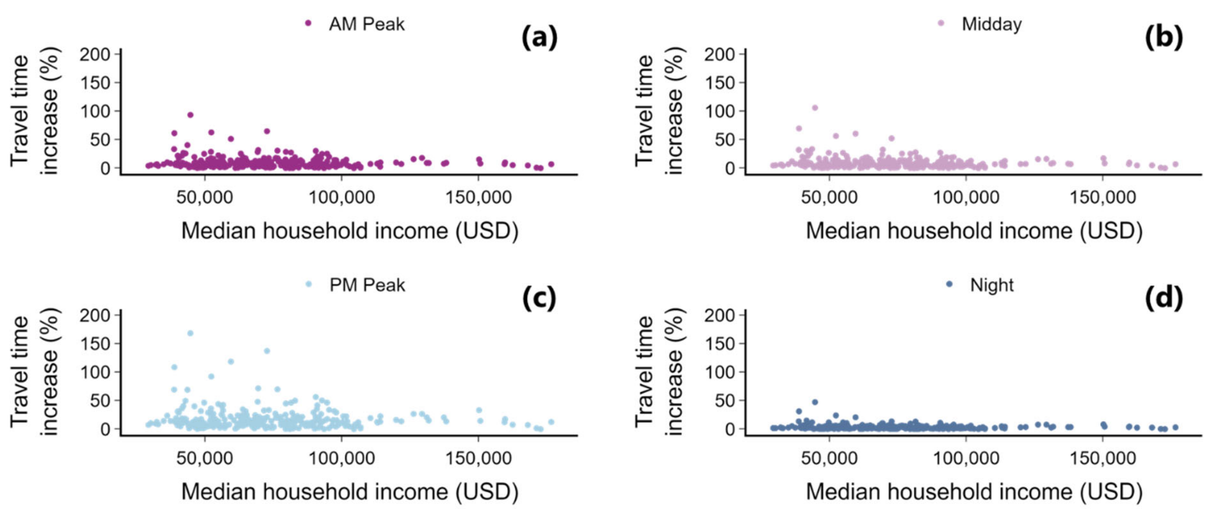

Figure S14. Block groups' median household income and non-flooding period travel time increase percentages over the free flow scenario when (a) the morning peak time, (b) the midday off-peak time, (c) the evening peak time, and (d) the night off-peak time. Refer to Figure S13 for other visualization details.

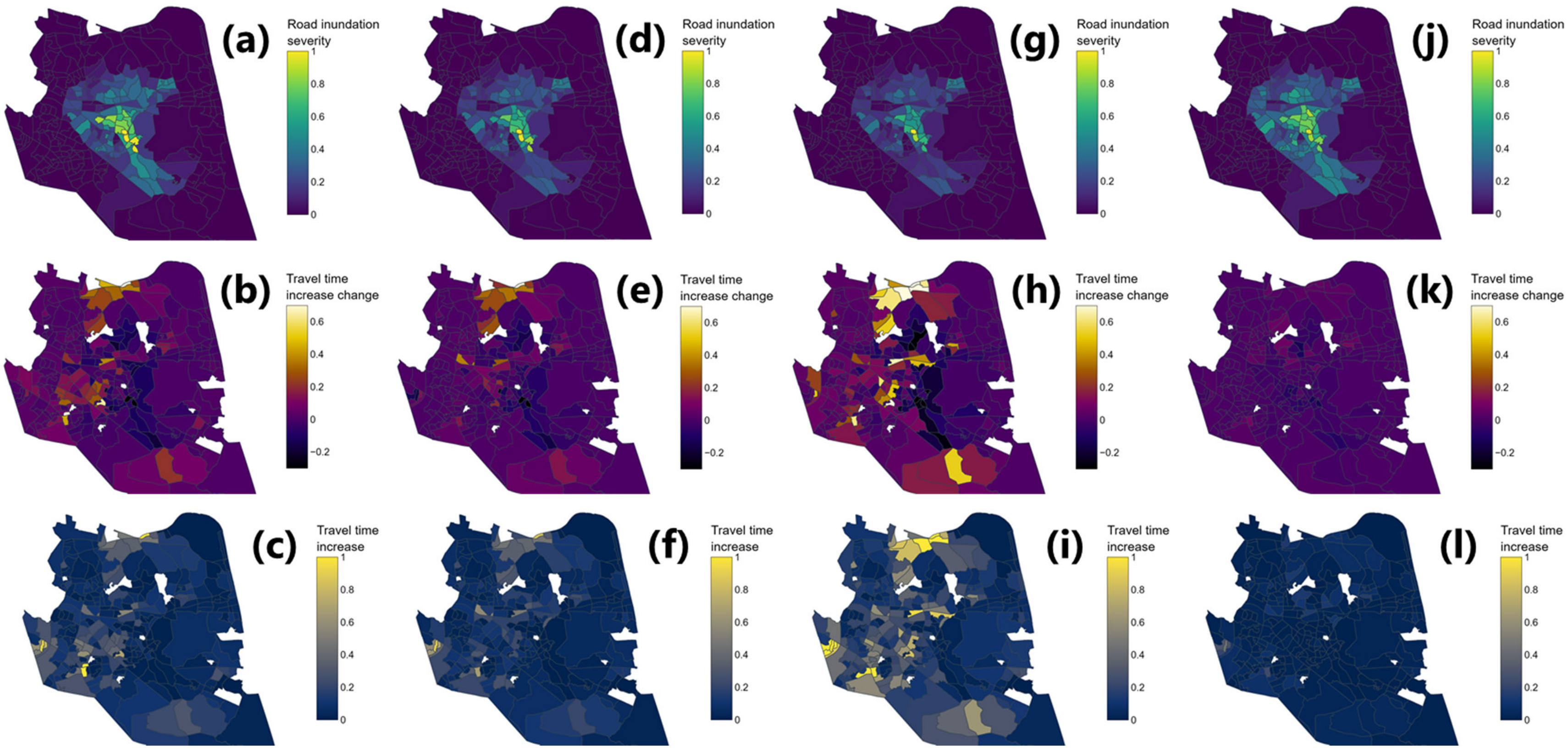

Figure S15. Block groups' road inundation severity, the cascading travel time increase percentage over the daily congestion scenario, and the flooding day travel time increase percentages over the free flow scenario, when (a-c) the morning peak time, (d-f) the midday off-peak time, (g-i) the evening peak time, and (j-l) the night off-peak time. Travel time increase percentages over one were visualized as one for consistency with the inundation severity's legend.

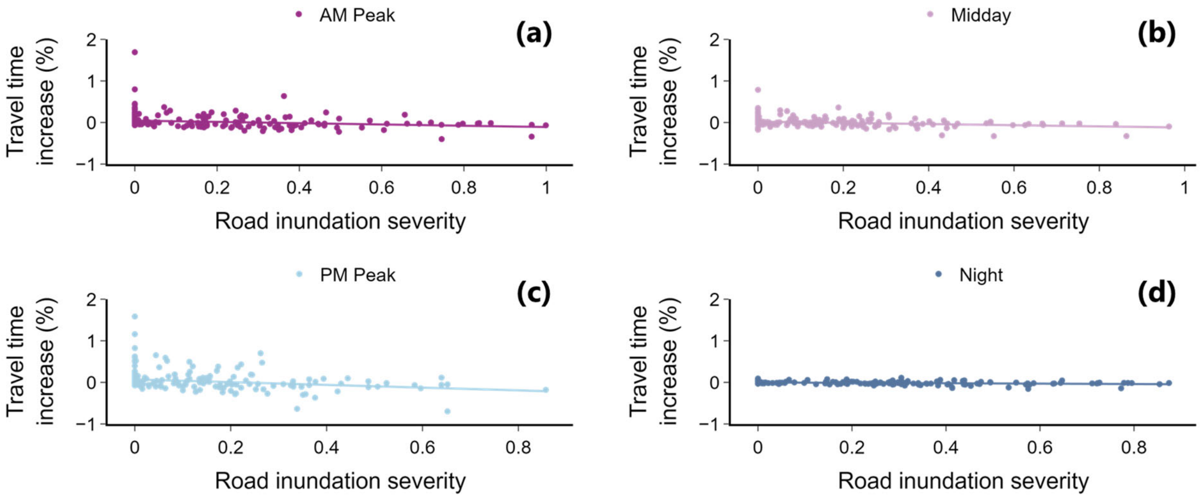

Figure S16. Block groups' road inundation severity and the flooding day travel time increase percentages over the free flow scenario when (a) the morning peak time, (b) the midday off-peak time, (c) the evening peak time, and (d) the night off-peak time. Refer to Figure S13 for other visualization details.

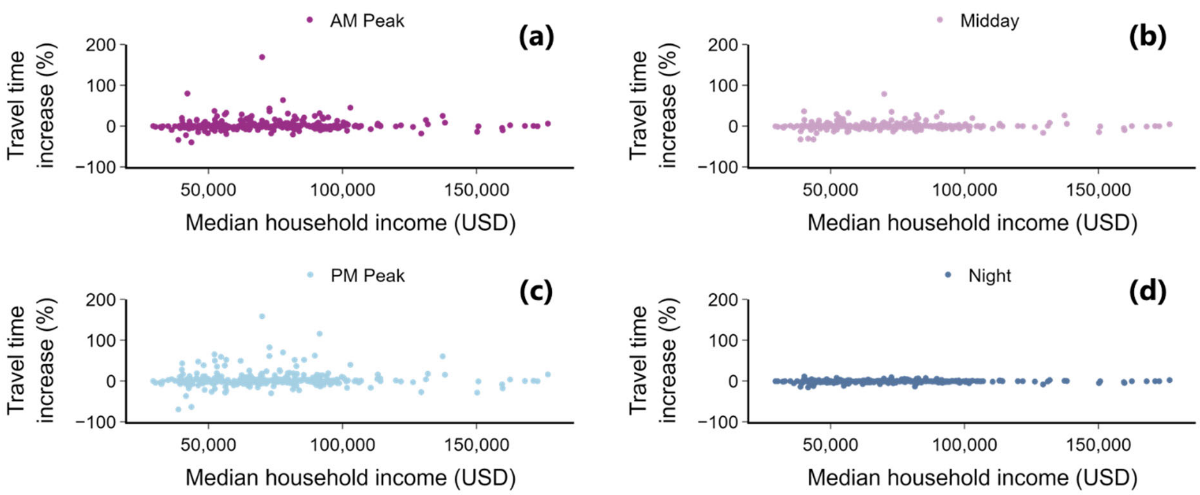

Figure S17. Block groups' median household income and flooding day travel time increase percentages over the daily congestion scenario when (a) the morning peak time, (b) the midday off-peak time, (c) the evening peak time, and (d) the night off-peak time. Values on the y-axis are the differences between those in Figure S13 and Figure S14. Refer to Figure S13 for other visualization details.

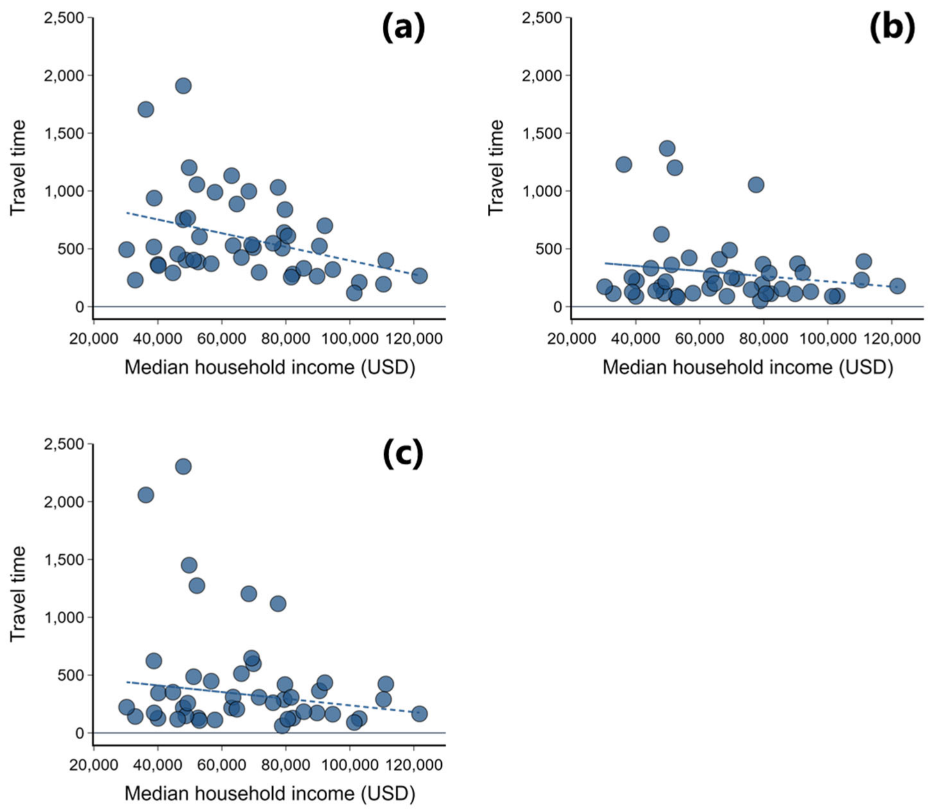

Figure S18. Income versus travel time for each block group using (a) the real-world dataset, (b) the state-of-the-art estimation method (i.e., Mode 2 in Table S2), and (c) the estimation method with recorded rescue station origins and flooding day traffic congestion modeling. The trend lines were based on coefficients in the spatial lag regression models. Details of the regressions are the same as those in Table 1.

Supplementary Tables:

Table S1. Summary of the modeling details in prior studies.

	Flood modeling		Road network					Routing				
Ref.	Flood incidents	Modeling method	One-way restriction	Speed limit[1]	Speed reduction[2]	Turn restriction	Cutoff threshold[3]	Objective	Traffic status[4]	Origin selection	Software	Risk metrics
1	March 2011, Ginosa, Italy	Hydrodynamics simulations	No	No	No	No	Stability model	Shortest path	No	N/A[5]	N/A	Route-based service metrics
2	2014, and 2015, York, U.K.	Hydrodynamics simulations	Yes	Yes	No	Yes	25 cm	Quickest routing	No	Minimal routing time	ArcGIS	Travel time; service area
3	100 and 500-year flood scenarios, New York City, NY	Hydrodynamics simulations	No	Yes	No	Yes	50 cm	Quickest routing	Yes	Minimal routing time	ArcGIS	Service area
4	20, 100, and 1000-year flood scenarios, Leicester City, U.K.	Hydrodynamics simulations	Yes	Yes	No	Yes	25 cm	Quickest routing	No	Minimal routing time	ArcGIS	Service area
5	October 2013 event, Galluzzo, Florence, Italy	Hydrodynamics simulations	No	Yes	Yes	No	30 cm	Quickest routing	No	Minimal routing time	N/A	Service area
6	5, 20, and 100-year flood scenarios, Shanghai, China	Hydrodynamics simulations	No	Yes	Yes	No	30 cm	Quickest routing	Yes	Minimal routing time	ArcGIS	Service area
7	100-year flood and 2013 flood, Calgary, Alberta	Elevation-based estimation	Yes	No	Yes	No	30 cm	Quickest routing	No	Minimal routing time	ArcGIS	Service area; served population
8	Hurricane Harvey, Houston County, TX	Hydrodynamics simulations	No	Yes	Yes	No	61 cm	Quickest routing; shortest path	No	N/A	N/A	Service loss
9	1-in-100-years surface-water flood, England	Flood risk maps	Yes	Yes	No	Yes	30 cm	Quickest routing	Yes	Minimal routing time	N/A	Service area; travel time

10	100 and 500-year flood, 24 cities in Iowa State	Flood risk maps	No	No	No	No	N/A	Shortest path	No	Minimal geometric distance	QGIS	Travel distance
11	2018 floodwave; Barotse Floodplain, Zambia	Hydrodynamics simulations	No	Yes	Yes	No	50 cm or 1.0 m s^{-1}	Quickest routing	No	N/A	QGIS	Travel time; service area; served population
12	100-year flood, Delaware	Hydrodynamics simulations	No	Yes	Yes	No	30 cm	Quickest routing	No	Minimal routing time	NetworkX	Travel time
13	100 and 1000-year flood, Shanghai, China	Hydrodynamics simulations	No	No	No	No	30 cm	Shortest path	No	Minimal routing distance	N/A	Route-based service metrics
14	Global recorded floods	Flood risk maps	No	Yes[6]	No	No	N/A	Quickest routing	No	N/A	N/A	Travel time
15	Precipitation days, Beijing, China	Precipitation	No	Yes[6]	Yes	No	N/A	Quickest routing	Yes	Minimal routing time	ArcGIS	Travel time; service area; served population
16	Typhoon In-Fa, Shanghai, China	Hydrodynamics simulations	No	Yes	Yes	No	N/A	Quickest routing	No	Minimal routing time	N/A	Route-based service metrics
17	50-year flood, Wuhan, China	Hydrodynamics simulations	No	Yes[7]	Yes	No	30 cm	N/A	Yes	N/A	ArcGIS	Extended travel time
18	Heavy rainfall on July 19, 2023, Nanjing, China	Social media posts; water gauge sensors	No	Yes	No	No	N/A	Quickest routing	No	Minimal routing time	N/A	Route-based service metrics
19	Super Typhoon Mangkhut, Pearl River Delta	Hydrodynamics simulations	No	No	Yes	No	30 cm	Quickest routing	No	Minimal routing time	ArcGIS	Service areas
Ours	Hurricane Matthew 2016, Virginia Beach, U.S.	Hydrodynamics simulations	Yes	Yes	Yes	Yes	30 cm	Quickest routing	Yes[8]	Minimal routing time	ArcGIS	Travel time; service areas

[1] If vehicle speed is set according to the speed limit when the road is not inundated. [2] If vehicle speed is reduced when the road is inundated but not closed. [3] The inundation depth threshold or water flow velocity threshold for road closure. [4] If traffic status (i.e., congestions) was considered in the modeling. [5]N/A: Not mentioned or not applied. [6]Average speed was used. [7] Observed speed was used. [8] Some prior studies considered traffic congestion using observed traffic speed. It is not easily doable in the use case of estimating future traffic status and flood

risk. Other studies considering traffic congestion reduced travel speeds based on what-if scenarios and did not aim to estimate congestion. The baseline implementation in the present study followed most of the prior studies and did not estimate traffic congestion, while congestions were used in the *Traffic congestion patterns and underestimation inequality* section.

Table S2. Regression results between median household income and emergency service travel time. Travel time is the dependent variable and income is the independent variable. The spatial lag regression model and the model setting the same as that in Table 1 were used.

Index	Mode	Origin	Congestion	Slope	p-value
1	Real-world	N/A	N/A	-0.00591*	0.01607
2	Estimate	Nearest	No	-0.00224	0.27217
3	Estimate	Recorded	Flooding	-0.00288	0.31377

Table S3. Accuracy metrics for different model settings. Mean Absolute Error (MAE) $= \frac{1}{n}\sum_{i=1}^{n}|y_i - \widehat{y_i}|$, Mean Absolute Percentage Error (MAPE) $= \frac{100\%}{n}\sum_{i=1}^{n}\left|\frac{y_i-\widehat{y_i}}{y_i}\right|$, Root Mean Squared Error (RMSE) $= \sqrt{\frac{1}{n}\sum_{i=1}^{n}(y_i - \widehat{y_i})^2}$, and bias $= \frac{1}{n}\sum_{i=1}^{n}(\widehat{y_i} - y_i)$, where n is the number of EMS incidents in the flooding day, y_i is the i^{th} ground truth value, y_i is the estimated travel time, $\overline{y}$ is the mean of ground truth values, and $\overline{\widehat{y_i}}$ is the mean of estimates. Row Five is the metrics of the model setting after considering the factors studied in the paper.

Index (n)	Period	Origin	Congestion	MAE (s)	MAPE (%)	RMSE (s)	Bias (s)
0	Non-flooding	Nearest	No	200.48	52.57	289.19	-191.99
1	Flooding	Nearest	No	381.83	51.88	627.49	-350.98
2	Flooding	Recorded	No	396.86	54.08	641.26	-339.54
3	Flooding	Nearest	Daily	366.67	49.17	603.73	-305.03
4	Flooding	Nearest	Flooding	341.51	47.48	576.26	-236.21
5	Flooding	Recorded	Flooding	**339.10**	**47.10**	**574.83**	**-233.80**

References

1. Albano, R., Sole, A., Adamowski, J. & Mancusi, L. A GIS-based model to estimate flood consequences and the degree of accessibility and operability of strategic emergency response structures in urban areas. *Natural Hazards and Earth System Sciences* **14**, 2847–2865 (2014).
2. Coles, D., Yu, D., Wilby, R. L., Green, D. & Herring, Z. Beyond 'flood hotspots': Modelling emergency service accessibility during flooding in York, UK. *J Hydrol (Amst)* **546**, 419–436 (2017).
3. Yin, J., Yu, D., Lin, N. & Wilby, R. L. Evaluating the cascading impacts of sea level rise and coastal flooding on emergency response spatial accessibility in Lower Manhattan, New York City. *J Hydrol (Amst)* **555**, 648–658 (2017).
4. Green, D. *et al.* City-scale accessibility of emergency responders operating during flood events. *Natural Hazards and Earth System Sciences* **17**, 1–16 (2017).
5. Arrighi, C., Pregnolato, M., Dawson, R. J. & Castelli, F. Preparedness against mobility disruption by floods. *Science of the Total Environment* **654**, 1010–1022 (2019).
6. Yin, J., Yu, D. & Liao, B. A city-scale assessment of emergency response accessibility to vulnerable populations and facilities under normal and pluvial flood conditions for Shanghai, China. *Environ Plan B Urban Anal City Sci* **0**, 239980832097130 (2020).
7. Tsang, M. & Scott, D. M. An integrated approach to modeling the impact of floods on emergency services: A case study of Calgary, Alberta. *J Transp Geogr* **86**, 102774 (2020).
8. Gori, A. *et al.* Accessibility and Recovery Assessment of Houston's Roadway Network due to Fluvial Flooding during Hurricane Harvey. *Nat Hazards Rev* **21**, 04020005 (2020).

9. Yu, D. *et al.* Disruption of emergency response to vulnerable populations during floods. *Nat Sustain* **3**, 728–736 (2020).
10. Alabbad, Y., Mount, J., Campbell, A. M. & Demir, I. Assessment of transportation system disruption and accessibility to critical amenities during flooding: Iowa case study. *Science of the Total Environment* **793**, 148476 (2021).
11. Mroz, E. J. *et al.* Impacts of seasonal flooding on geographical access to maternal healthcare in the Barotse Floodplain, Zambia. *Int J Health Geogr* **22**, 1–20 (2023).
12. Gangwal, U., Siders, A. R., Horney, J., Michael, H. A. & Dong, S. Critical facility accessibility and road criticality assessment considering flood-induced partial failure. *Sustain Resilient Infrastruct* **8**, 337–355 (2023).
13. Shan, X. *et al.* Deficiency of Healthcare Accessibility of Elderly People Exposed to Future Extreme Coastal Floods: A Case Study of Shanghai, China. *International Journal of Disaster Risk Science* **14**, 840–857 (2023).
14. Mühlhofer, E., Bresch, D. N. & Koks, E. E. Infrastructure failure cascades quintuple risk of storm and flood-induced service disruptions across the globe. *One Earth* **7**, 714–729 (2024).
15. Zhang, Y. *et al.* Spatial accessibility of emergency medical services under inclement weather: a case study in Beijing, China. *Natural Hazards and Earth System Sciences* **24**, 63–77 (2024).
16. Zheng, M., Liu, J., Gao, J., Zhou, N. & Jiang, S. Navigating urban challenges: Quantifying emergency service accessibility and robustness amid meteorological disasters. *International Journal of Disaster Risk Reduction* **110**, 104655 (2024).
17. Chen, H. *et al.* Enhancing flood-response commuting resilience via driving mechanism investigation: New evidence from Wuhan, China. *Travel Behav Soc* **35**, 100743 (2024).

18. Zhu, S., Jiang, Y. X., Zhang, J., Dai, Q. & Yang, X. Evaluating the effect of urban flooding on spatial accessibility to emergency shelters based on social sensing data. *Transactions in GIS* **28**, 23–39 (2024).

19. Zhang, Z. *et al.* A cross-scale modeling framework for simulating typhoon-induced compound floods and assessing the emergency response in urban regions. *Ocean Coast Manag* **245**, (2023).